Phenomenology of K^+-nucleus scattering

C. M. Chen
Saint John's and Saint Mary's Institute of Technology, Tam-Sui, Taipei County, Taiwan 25135, Republic of China

D. J. Ernst
Department of Physics and Astronomy, Vanderbilt University, Nashville, Tennessee 37235

Mikkel B. Johnson
Los Alamos National Laboratory, Los Alamos, New Mexico 87545

(Received 13 July 1998)

A density expansion of the K^+-nucleus optical potential is used within a momentum-space approach to analyze the experimental total and elastic differential cross section data. We add to the microscopic first-order optical potential a phenomenological higher-order term proportional to the nucleon density raised to a power α. A fit to the total cross section data yields a value for α of 2.85 ± 0.25 and a strength for the potential that decreases slightly faster than the inverse of the kaon laboratory momentum. To obtain a higher-order potential compatible with all the data and with parameters that are target independent, a renormalization of the differential cross section data by 30%, consistent with our estimate of systematic errors, is made. The need for such a large renormalization is explained. [S0556-2813(99)04105-9]

PACS number(s): 25.80.Nv, 24.10.Eq, 24.10.Jv

I. INTRODUCTION

The properties of a hadron (such as its mass, radius, or scattering cross sections with various probes) are expected to be modified in a nucleus. At low densities, these are the same as the properties in free space, but as the density increases the effects of the medium will become increasingly important. The quantitative characterization of these medium effects is basic to the understanding of strong interaction dynamics and is of particular interest to, but not limited to, the understanding of the role of quantum chromodynamics (QCD) in nuclear physics. The unusually large higher-order effects found here for the K^+-nucleus reaction are a tantalizing indication of an underlying phenomena which could shed some light on these matters. However, an understanding of the missing physics still awaits additional data and more detailed and predictive models.

The properties of a hadron in the nucleus can be studied in a scattering experiment. The K^+ is uniquely important in this regard because of all hadrons it penetrates most deeply into a nucleus. K^+-nucleus total, reaction, elastic, inelastic, and quasielastic cross section data [1–3] are all relevant for these studies, which confirm [4,5] an enhanced K^+-nucleon scattering for a nucleon embedded in the nuclear medium. One expects the enhancement to evolve with increasing nuclear density; the details should provide insight into the underlying mechanism, which is not understood at the present time. A phenomenological determination of the density dependence may be obtained by modeling results from a variety of nuclear targets using a density expansion of the hadron-nucleus interaction. This expectation is based on the relatively weak K^+ interaction: the K^+ can penetrate to densities approaching normal nuclear matter density (about 0.16 nucleons/fm^3) for a medium-mass target such as ^{40}Ca, yet it probes relatively low densities for a light nucleus like ^{6}Li.

An analysis of the K^+ data using an effective interaction exists [6], but it is not of a form that permits the extraction of the density dependence. It is the goal of this work to extract the relevant parameters of the density dependence of the higher-order K^+-nucleus interaction, specifically the power of the density with which it varies and the strength of its coupling.

The ratio R of the kaon-nucleus total cross section to that for the deuteron,

$$R = \frac{2\sigma_A}{A\sigma_D}, \tag{1}$$

is sensitive to important features of the interaction. For light nuclei such as ^{6}Li and ^{12}C, this ratio is experimentally greater than one. On the other hand, all existing theoretical calculations give $R<1$ by a small amount. The first-order theory predictions are necessarily smaller than one as a simple result of nucleon shadowing, i.e., some of the nucleons are hidden behind other nucleons. For ^{12}C, shadowing amounts to a 10% correction. All calculations are in agreement because the optical potential, for an interaction as weak and nearly energy independent as the K^+-nucleon interaction, is reasonably well approximated by the on-shell t matrix times the density. Even making a change as dramatic as replacing the Klein-Gordon by the Kemmer-Duffin-Petiau [7] propagator has little effect [3]. The discrepancy between the data and the theory is thus not only theory independent but its existence does not even seem to depend on the details of the theory.

Several explanations have been put forth for the physical origin of the discrepancy in R. They include an increase in the physical size of the nucleon [8] in the nuclear medium, enhanced mesonic exchange currents caused by medium modifications of mesonic masses [9], medium modifications to the mesons being exchanged between the kaon and the target nucleon treated as a Dirac particle [10], or a combina-

tion of correlation effects and meson currents [11]. A calculation of conventional meson exchange currents [12] shows that these are too small to be an explanation of the discrepancy. A thorough examination of the dependence of physical observables on the magnitude of the in-medium enhancement of the kaon-nucleon amplitude can be found in [13].

Here we examine the total and differential cross section data of Refs. [2,3] using a phenomenological analysis. The data of [2] consists of total cross sections on four targets, ^{6}Li, ^{12}C, ^{28}Si, and ^{40}Ca, at four laboratory momenta, 488, 531, 656, and 714 MeV/c. The elastic differential cross sections [3] consist of data for ^{6}Li and ^{12}C at 714 MeV/c. To reduce the uncertainty in the normalization of the total cross sections (in both the data and the theoretical calculations), we analyze the ratio R as defined by Eq. (1).

In the next section, we describe the model. In the following section, we examine the implications of the total cross section measurements. In Sec. IV, the differential cross sections are included in the analysis. Finally, a summary of this work is given in Sec. V.

II. MODEL

For the theoretical analysis, we utilize the momentum-space optical model of Ref. [14]. There are many reasons for utilizing the momentum-space approach. These include (1) fully covariant kinematics, normalizations, and phase-space factors [15], (2) relativistically invariant amplitudes [16], (3) the crossing symmetric Klein-Gordon propagator [17], and (4) an exact evaluation of the fermi averaging integral. A review of the approach can be found in [5].

The first-order potential is the leading term of a systematic, formal expansion of the full optical potential in powers of the nuclear density matrix [18]. This expansion, called the hole-line expansion, is a convenient theoretical bookkeeping representation of meson-nucleus reaction dynamics. While the first-order potential is essentially completely conventional in character, the higher-order terms may contain exotic as well as conventional physics.

In the case of pions [18,19], the mechanisms contributing to the higher-order terms appear to be completely conventional in character, and, in addition, the expansion converges rapidly for the purpose of calculating elastic scattering from nuclei up to several hundred MeV of incident pion kinetic energy. In this case, the main correction is the second-order optical potential, which is adequately approximated in the local-density approximation, i.e., may be taken to depend on the square of the nuclear density.

For the case of kaons, we are motivated by the success of the hole-line expansion for pions, and we add to the microscopic lowest-order optical potential a purely phenomenological higher-order potential proportional to a power α of the nuclear density. In momentum space its form is

$$\langle \vec{k}' | U^{(2)} | \vec{k} \rangle = \frac{\lambda}{\rho_0} \rho^{(\alpha)}(\vec{k}' - \vec{k}), \tag{2}$$

where $\rho^{(\alpha)}(\vec{q})$ is the Fourier transform of the nuclear density to the α power,

TABLE I. The results from fitting the A dependence of the total cross section ratio R, Eq. (1), at four different energies. The value of χ^2 for each fit, the strength of the second-order optical potential Im λ, and the power of the density α [see Eq. (2)] are given.

$k_{\rm lab}$ (MeV/c)	T_K (MeV)	χ^2	α	Im λ(fm$^{5.4}$)
488	200	0.33	2.7 ± 0.8	0.209 ± 0.023
531	231	5.04	3.9 ± 0.8	0.154 ± 0.065
656	327	3.73	2.9 ± 0.4	0.165 ± 0.007
714	374	7.77	2.6 ± 0.4	0.125 ± 0.005

$$\rho^{(\alpha)}(\vec{q}) = \frac{1}{(2\pi)^3} \int [\rho(\vec{r})]^{\alpha} e^{i\vec{q}\cdot\vec{r}} d^3r. \tag{3}$$

Here ρ_0 is the density of nuclear matter, 0.16 fm^{-3}, so the units on λ are fm to the $3(\alpha-1)$ power. The normalizations follow Ref. [14]. Since we do not know as much about the underlying dynamics for kaons, we allow α to be a variable whose value is determined by the data. If the dynamics is conventional, we expect $\alpha=2$ (although unconventional dynamics could also appear with this power of density), whereas $\alpha>2$ would indicate the dominance of multinucleon processes, suggesting physics of an exotic, or at least of a less than conventional, nature. Since we are varying the power α, our model consists of three parameters to be determined from the data, one complex number λ and one real parameter, α.

III. TOTAL CROSS SECTIONS

We first analyze the total cross section data of Ref. [2]. The large uncertainties introduced by the systematic errors in the measurement of an individual cross section are reduced by taking the ratio R of the total cross section to that of the deuteron defined in Eq. (1), where both cross sections are measured with the same beam and the same detector during the same experiment. Similarly, the errors in the theory are reduced by addressing this ratio [20]. The theoretical cross sections for the deuteron are calculated in momentum space following Ref. [21]. The total cross sections are found to be very insensitive to Re λ, so for our analysis of the total cross section data we first restrict the parameters of the fit to the meaningful set, Im λ and α.

We begin by examining each energy independently. At each energy we assume that a single value of Im λ and α will provide an adequate description of the target dependence given by the four measured nuclei. The results are given in Table I. Note that the values of α determined from this procedure are reasonably energy independent. The best-fit value for α as fit to the individual values determined at each energy is $\alpha=2.85\pm0.25$, where the error represents one standard deviation.

In Figs. 1–4 we show the A dependence of the ratio R for each energy compared to the experimental data. The curves indicate the sensitivity to the density dependence; they correspond to theoretical calculations for $\alpha=2.85$, $\alpha=2.85+0.25$, $\alpha=2.85-0.25$, and $\alpha=2.0$, where Im λ is readjusted for each curve to give the best possible fit. We learn several things from these figures. First, a quadratic density dependence for the second-order potential is not at all ad-

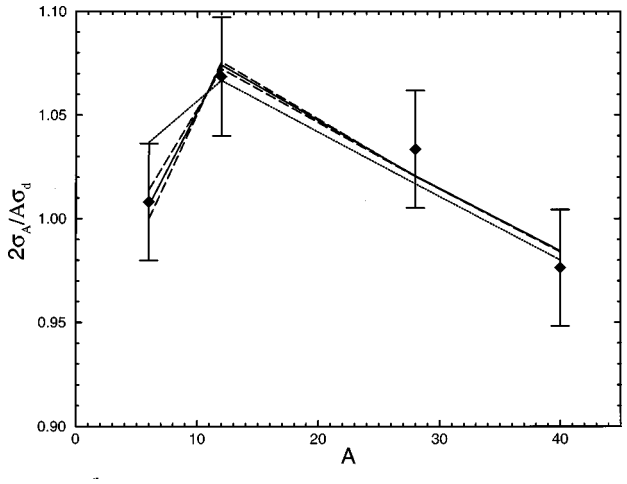

FIG. 1. The total cross section ratio R versus atomic mass A for kaon laboratory momentum $k_{\rm lab}=488$ MeV/c. The data are from Ref. [2] and the targets are ^{6}Li, ^{12}C, ^{28}Si, and ^{40}Ca. The solid curve is the theoretical result for a second-order potential as defined in Eq. (2) with $\alpha=2.85$. The dashed curves are for $\alpha=2.85+0.25=3.10$ and $\alpha=2.85-0.25=2.60$. The dotted curve is for the potential proportional to the density squared, $\alpha=2.0$. In all cases, the strength of the potential Im λ is varied to produce the best possible fit.

equate. On the other hand, the best-fit value $\alpha=2.85\pm0.25$ does produce reasonable results on average.

The value of α is fixed dominantly by the difference between ^{6}Li and ^{12}C. Note that the low value of the ^{6}Li cross section at 531 MeV/c is giving a higher value of α at this one energy. We also see that the heavier nuclei are insensitive to the value of α. The reason for this is that although the K^+ nucleon is weak on the scale of a strong amplitude, the kaon cannot penetrate all the way through a nucleus such as ^{28}Si or ^{40}Ca [22]. Thus the density to which the scattering is most sensitive is determined by the two-body amplitude and the penetrability that it allows. The effective density does not vary from target to target for these heavier nuclei. The decrease in R with increasing A is the result of shadowing. As the size of the nucleus increases, a somewhat smaller fraction of the total number of nucleons are visible to the kaon. The theory reproduces this phenomenon quite well.

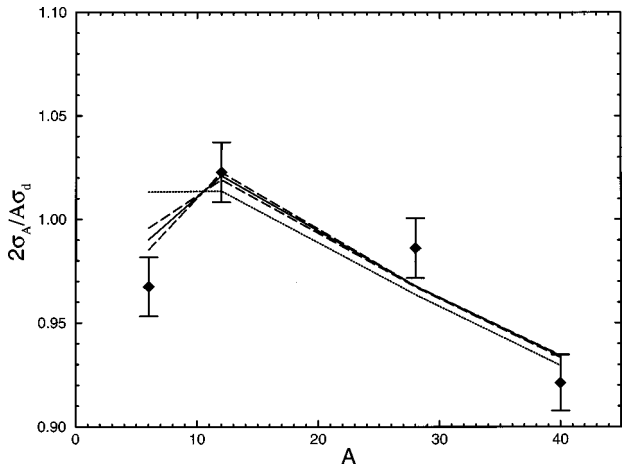

FIG. 2. The same as Fig. 1 except $k_{\rm lab}=531$ MeV/c.

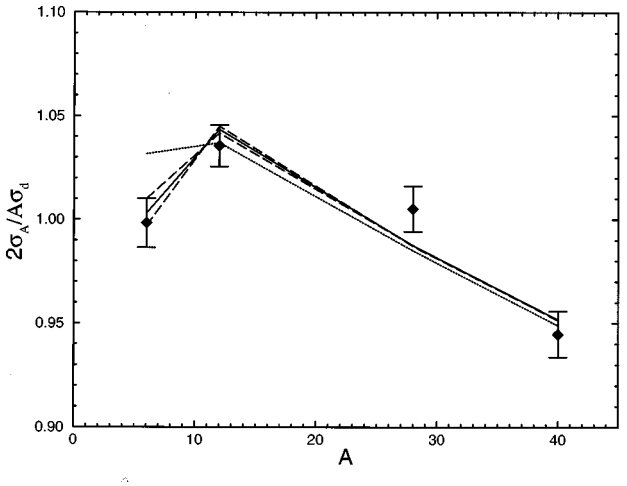

FIG. 3. The same as Fig. 1 except $k_{\rm lab}=656$ MeV/c.

In Table I we also give the value of λ determined by a best fit with α fixed at 2.85. For a conventional second-order correction, a rough estimate for the magnitude of the correction [23] gives a value directly proportional to a length scale (the correlation length for correlation corrections), the density squared, and the two-body total cross section σ_{KN}, and inversely proportional to the meson momentum k_0. The energy dependence of the second order would then be expected to be proportional to σ_{KN}/k_0. The total cross section (averaged over proton and neutron) σ_{KN} is rather constant over this energy range. It goes from 12.9 mb at 488 MeV/c to 14.3 mb at 714 MeV/c, indicating only an 11% increase. Thus we would expect the k_0^{-1} to dominate and produce a decreasing second-order interaction. Within the rather large fluctuations in the values of Im λ, we see a decrease in Im λ that is slightly more rapid then k_0^{-1}. There is certainly nothing exotic in the energy dependence of Im λ.

IV. DIFFERENTIAL CROSS SECTIONS

In [24] it was observed that for low-energy kaons and for pions in the GeV range of energies there is sufficient Coulomb-nuclear interference to be able to extract in a model independent way both the real and imaginary parts of

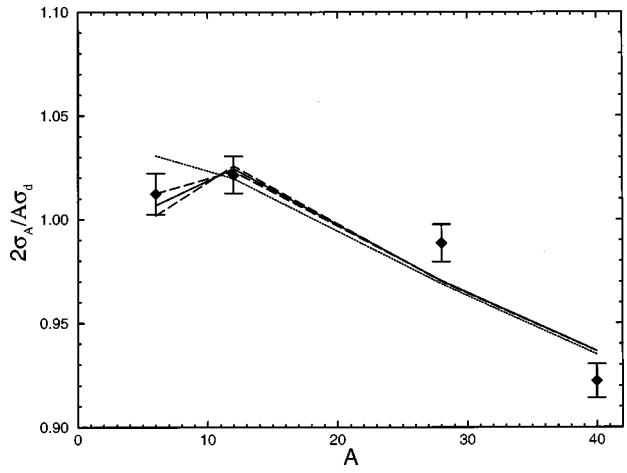

FIG. 4. The same as Fig. 1 except $k_{\rm lab}=714$ MeV/c.

the forward strong-interaction scattering amplitude from the differential cross section data alone. As the imaginary part of this amplitude is also related to the total cross section through the optical theorem, the use of both differential and total cross sections provides a means of assessing the consistency of the different data sets and thus improving confidence in the analysis for the real part of the forward elastic-scattering amplitude. From the real part of the scattering amplitude, one may then determine Re λ, whose value is an independent source of information for understanding the origin of the medium effects. For the data available, the procedure of Ref. [25] worked well [24] for pions, but for kaons the more limited data necessitated additional assumptions to obtain the forward-scattering amplitudes. In our current work, by utilizing a model for the first- and second-order optical potential and including the total cross section data, we are able to improve this analysis.

We now consider the differential cross sections for ^{6}Li and ^{12}C at 714 MeV/c taken from Ref. [3], in addition to the total cross sections. We use the differential cross section data for angles less than 25 degrees only, and we fit these points together with the total cross sections. We limit ourselves to forward-angle data because the overall strength of the optical potential and its range are determined primarily by the forward scattering data, whereas more subtle issues are involved in the details of the differential cross section at larger angles, as we discuss below.

We incorporate the systematic error in the differential cross section by treating its normalization N as an independent parameter to be varied in the χ^2 fit to the data. The contribution of N to χ^2 is given by $\chi^2_{\rm Norm}$ given by

$$\chi^2_{\rm Norm}=\frac{(1-N)^2}{\Delta N^2}, \tag{4}$$

where ΔN is the error in the normalization. The systematic error for the differential cross sections is 15%. There is also a 15% error in the theoretical calculations arising from the error in the experimental two-body amplitudes [26] that are used as input. Since we are interested in the relative size of the theory compared to the experiment, we add these two errors in quadrature to give an effective 21% for ΔN.

In addition, there is also an error associated with the analysis of the transmission experimental data, from which the total cross section is determined by an extrapolation of data to zero solid angle. This error arises from the large Coulomb-nuclear interference in the forward direction and the necessity of introducing a model to extrapolate through it. The most consistent approach [27,6] would, of course, be to use our own model of elastic scattering to perform this extrapolation, but we estimate the error introduced by not doing so is only about 5%. Thus, we adopt the simpler procedure of using the total cross sections from the experimental paper and adding this 5% to the quoted systematic error ΔN. This gives an effective systematic error of 22%. That this is an adequate procedure is verified by fitting two different values of the total cross section extracted from the same data as in [2] and [6] and finding that our results change only at the few percent level.

For ^{6}Li we ignore the quadrupole contribution to the elastic scattering. It was shown in Ref. [28] that this is a negligible contribution to the elastic scattering. In addition, we find that a meaningful fit requires that we include additional systematic errors in the differential cross section above and beyond the small statistical errors given in [2]. These arise because the resolution in the spectrometer was such that not only the elastic final state was included in the raw data but also several low-lying excited states. The contribution of these excited states to the data can be removed using a model for the elastic and inelastic scattering to the measured data. A preliminary analysis [28] indicates that the results in [3] will change somewhat if additional excited states are included in this correction. There is thus some amount of additional uncertainty in the precise shape of the differential cross section. This both provides further motivation to concentrate on the forward angle points where these corrections are smallest and also requires either adding some estimated error to the differential cross sections or equivalently enhancing the importance given to the measured ratio R of the total cross section. We have chosen to reduce the error assigned to the total cross sections thus forcing a good fit to these measurements. We find this is roughly equivalent to assigning the differential cross sections an additional error of about 10%.

We employed two separate fitting procedures. In the first procedure, we fit the differential cross sections together with the total cross section datum at 714 MeV/c for the two nuclei ^{12}C and ^{6}Li. We vary the values of λ and N separately for each nucleus, fixing α at its best-fit value, $\alpha=2.85$. Fitting the parameters separately for these two nuclei gives insight into the interplay between the data (total cross section and angular distributions) and the parameters of our model. However, since the resulting values of λ are different for the two nuclei in this procedure, we next fit using a *common* set of parameters λ and N but maintaining α at 2.85. We expand the data set to include the total cross sections for the complete set of nuclei ^{6}Li, ^{12}C, ^{28}Si, and ^{40}Ca. This final fit to the total data set at 714 MeV/c with values for λ and N that are independent of A provides the results for our model of the higher-order corrections.

The best fit values of λ and N in our first fitting procedure are given in Table II. For reasons discussed above, we have used the differential cross sections for angles less than 25 degrees. The real part of the forward scattering amplitude $F(0)$ presented is the difference between the full scattering amplitude and the finite-size Coulomb amplitude extrapolated to zero. It does not contain any additional modifications [25] that are designed to further remove Coulomb effects. We see that for ^{12}C the fit requires a renormalization of the differential cross section by $17\pm2\%$, which is well within our estimate of the total relative normalization between the theory and the data.

The fit for ^{6}Li is interesting. Notice in Fig. 5 that the experimental differential cross section data lies below the first-order theory for ^{6}Li, whereas the measured total cross section lies above [5] the theory. Fitting the total cross section data thus requires increasing the value of the imaginary part of λ. However, this will necessarily *increase* the theoretical differential cross section and therefore worsen the fit of this quantity to the data. To avoid contradiction, our fitting procedure raises the experimental differential cross section through the renormalization N, while lowering the theoretical differential cross section by forcing a cancellation of the real

TABLE II. The results of fitting the total cross section ratio and the forward angle differential cross section separately for ^{6}Li and ^{12}C at $k^{lab}=714$ MeV. The value of α has been fixed at 2.85. The strength of the second-order potential λ, the renormalization N of the differential cross section data, the experimental value of the cross section ratio R_{exp}, the cross section ratio that results from the theoretical fit R_{th}, and the extracted value of the real part of the forward scattering amplitude Re $F(0)$ are given.

Target	Re λ(fm$^{5.4}$)	Im λ(fm$^{5.4}$)	N	R_{exp}	R_{th}	Re $F(0)$(fm)
^{6}Li	0.593 ± 0.055	0.185 ± 0.004	1.16 ± 0.02	1.012 ± 0.010	1.012	-0.656
^{12}C	0.029 ± 0.005	0.127 ± 0.001	1.17 ± 0.02	1.022 ± 0.009	1.021	-2.01

part of the phenomenological higher-order potential against the real part of the first-order amplitude through a large value for Re λ, Re $\lambda=0.593\pm0.055$ fm$^{5.4}$. This cancellation is significant in spite of the large size of the imaginary part of λ, Im $\lambda=0.185\pm0.003$ fm$^{5.4}$. The required renormalization of the ^{6}Li differential cross section measurements is $16\pm2\%$ and is quite consistent with the value obtained for ^{12}C. Notice that the average value of Im $\lambda=0.13\pm0.01$ fm$^{5.4}$ is consistent with the value found from the total cross sections alone as given in Table I.

In the second fit, we expand the data set by including also the total cross section data for ^{28}Si and ^{40}Ca and assume that the parameters λ and N are independent of the target in accord with the hole-line expansion. The most noticeable difference for this fit is that the differential cross sections are renormalized by $30\pm2\%$, whereas in our first procedure a 17% renormalization was necessary. There is little penalty for making the large renormalization of the data needed to arrive at this solution because of the large systematic uncertainty. The resulting value of λ is given by Re $\lambda=-0.015\pm0.010$ fm$^{5.4}$ and Im $\lambda=0.124\pm0.0002$ fm$^{5.4}$. These are similar to the fit to ^{12}C alone.

Because of the large systematic uncertainty, our second fitting procedure is able to produce a solution quite different from that of the first, but one of comparable χ^2. Recall that in our first procedure, the fit to ^{6}Li entailed a cancellation of the higher-order potential against the first-order optical potential, whereas the fit to ^{12}C was acceptable without such a cancellation. For this reason we obtained a larger value of Re λ for ^{6}Li than for ^{12}C. In our second fitting procedure, where, according to the hole-line expansion, λ must have the same value for the two nuclei, the cancellation is no longer effective. Instead, the differential cross sections acquire a larger renormalization than they had before, placing the forward angle data for ^{6}Li *above* the first-order theory. The difference between the first-order theory and the (renormalized) data is now able to be repaired principally by the value of Im λ, which increases the theoretical forward-angle differential cross sections for all nuclei. In this fashion, there is no longer a need for a large value of Re λ, previously found for ^{6}Li but not for ^{12}C.

We would like to emphasize our finding that within the framework of the hole-line expansion, no choice of optical potential parameters can simultaneously fit the total cross sections and increase the differential cross section for ^{12}C without simulatneously increasing the differential cross section for ^{6}Li. For this reason, we believe that all theoretical models with a reasonable microscopic basis will be unable to reproduce the existing empirical cross section data without large renormalization of it, such as we have been forced to make. Precisely how this happens will depend on the model, but since we have chosen a quite general parametrization of the optical potenital, we expect no more than semiquantitative changes from the results of our study.

The theoretical results for the total cross sections are given in Fig. 6. The results are comparable to those in Fig. 4 where only the totals were fit utilizing one parameter, Im λ.

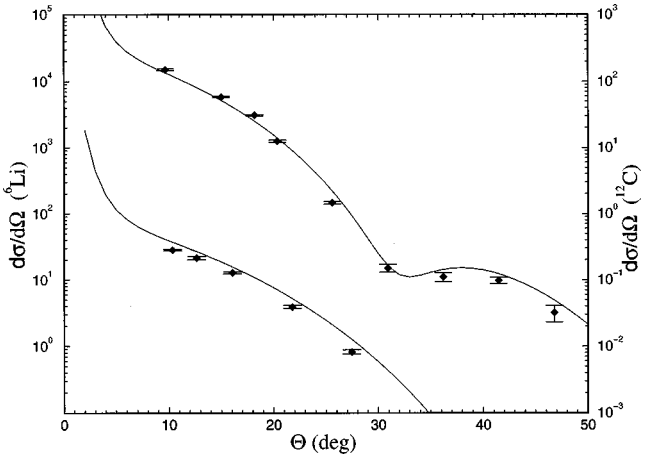

FIG. 5. The differential cross section for elastic scattering of K^+ from ^{6}Li and ^{12}C at $k_{lab}=714$ MeV/c versus scattering angle. The bottom curve is for ^{6}Li and goes with the left axis; the top curve is for ^{12}C and goes with the right axis. The data are from Ref. [3] and the curves are from the first-order momentum space optical model calculation.

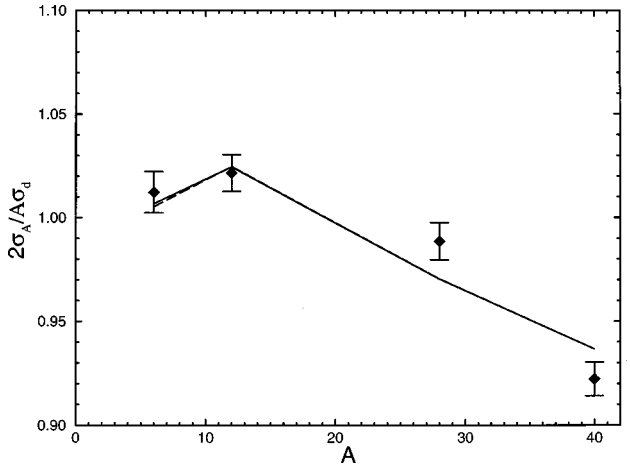

FIG. 6. The same as Fig. 4 except the curves result from a fit to this total cross section data and to the differential cross section data simultaneously.

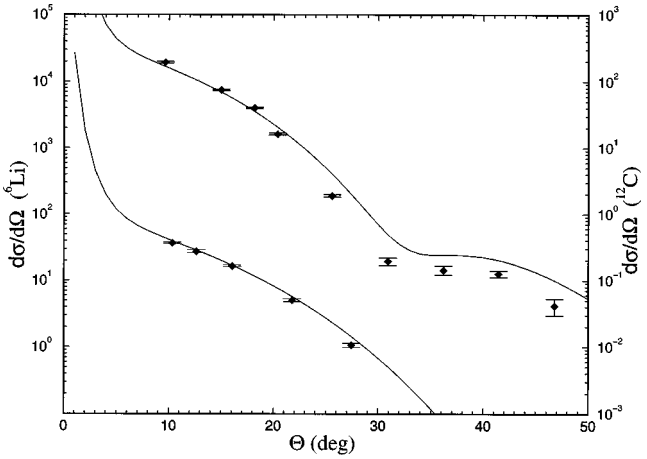

FIG. 7. The same as Fig. 5 except the data have been renormalized by 30% as resulted from the fitting process. The curves are from the momentum space optical model calculations and include the full second-order potential as defined in Eq. (2).

In Fig. 7 we present the differential cross sections. Here we plot the data with the 30% renormalization. These curves should be compared to the first-order curves given in Fig. 5. In Fig. 8 we present the ratio of the differential cross sections for ^{12}C to ^{6}Li. We see that the fit is a compromise to the magnitude of the ratio and that the shape is not reproduced quantitatively. The resulting values for R and $F(0)$ are given in Table III. The value of Re $F(0)$ changed significantly for both targets reflecting the change in normalization of the data. As explained above, the renormalization of the differential cross sections is a result of the qualitative features of the total cross section measurements and would be necessary for any analysis of the total body of data. We thus tend to believe the results of this analysis. However, a definitive value for $F(0)$ will require a well determined normalization for the differential cross section data.

The experimental total cross sections that result from the analysis of Ref. [6] are about 3% higher than those of Ref. [2] even though they utilize the same transmission data. If we repeat our analysis using these numbers for the total cross

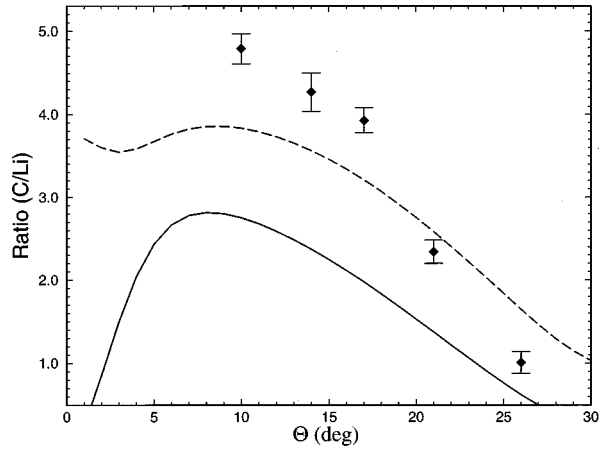

FIG. 8. The ratio of the differential cross section for ^{12}C to the cross section for ^{6}Li for $k_{\rm lab}=714$ MeV/c. The dashed curve is the first-order result while the solid curve includes the full phenomenologically determined second-order potential.

TABLE III. The results of fitting the total cross section ratios and the differential cross sections for ^{6}Li and ^{12}C simultaneously at $k_{\rm lab}=714$ MeV. The value of α has been fixed at 2.85. The cross section ratios given by the theory $R_{\rm th}$ and the real part of the forward scattering amplitude Re $F(0)$ are given.

Target	$R_{\rm exp}$	$R_{\rm th}$	Re $F(0)$(fm)
^{6}Li	1.012 ± 0.010	1.005	-1.05
^{12}C	1.022 ± 0.009	1.025	-2.23

sections, we find that the power α would decrease by about 0.1 to 0.2, that the renormalization of the differential cross sections would increase (for the final analysis from 30 to 38%), and that Im λ would increase similarly to Im $\lambda \cong 0.165$ fm[5,4].

Our philosophy is very different from that of Ref. [6], where an energy-independent and A-dependent ''second-order'' correction proportional to the density was used. In our case, the potential is instead energy dependent and A independent. To fit their potential to the data, they first adjust the imaginary part of the impulse approximation optical potential to fit ^{6}Li. The remainder of the nuclei then have the imaginary part of the optical potential further scaled by a factor proportional to $(\overline{\rho}-\rho_c)$, where $\overline{\rho}$ is the average nuclear density of the target and ρ_c is an adjustable parameter. The strong A dependence evident in Figs. 1–4 requires this factor to be strongly A dependent. In our work, by contrast, the variation of the cross sections with A arises purely from the dependence of the higher-order optical potential on the density. Because they have more parameters, their results produce more accurate fits to the data than our work.

We have investigated the possibility of adding an additional term to our phenomenology in order to improve the fit for angles greater than 25 degrees. We tried terms that were of the form $\vec{k}'\cdot\vec{k}$, $q^2=(\vec{k}'-\vec{k})^2$, $\cos\theta$, or $\cos^2\theta$, all times $\rho^{(\alpha)}$. We found that adding these terms did not significantly improve our results.

V. CONCLUSIONS

We have found that the strong A dependence of the total cross sections for ^{6}Li and ^{12}C indicate an energy-dependent higher-order potential that is proportional to the density to the 2.85 ± 0.25 power. This could be considered an indication of either an exotic mechanism or a slowly convergent multiple scattering theory where the power being larger than two is modeling significant third and higher-order corrections. This latter possiblility is also exotic in that the kaon-nucleon two-body amplitude is much weaker than other strong amplitudes so one would expect a more rapidly convergent theory, not one that converges more slowly. A more conventional energy-dependent potential proportional to the square of the density is clearly ruled out. In analyzing the total and forward angle differential cross sections for ^{6}Li and ^{12}C at 714 MeV/c for the strength of the potential, we find two solutions of comparable χ^2. Our different solutions amount to different means of accounting for an unusual feature of the data, namely the fact that the first-order theory under predicts the total cross section while it over-predicts the differential

cross section for ^{6}Li. The resulting second-order potential provides a phenomenological representation of this physics. When we analyze the angular distributions for ^{6}Li and ^{12}C separately, we find an important role for the real part of the optical potential and that a moderate, 17% renormalization of the differential cross section data is required. On the other hand, when we analyze the angular distributions simultaneously, the real part of the optical potential plays a much smaller role and we are able to find a comparable fit if we accept a 30% renormalization of the differential cross section data. (This renormalization is accounting for both the systematic uncertainty in the norm of the data and also the uncertainty in the overall norm of the theory.) In both procedures, a comparable value for the imaginary part of the higher-order optical potential is obtained, which in our model characterizes the underlying theory.

In order to better understand the missing piece of physics, charge-exchange data would add interesting additional information. Single charge exchange data on ^{3}He and ^{13}C, for example, would allow a phenomenological determination of the isospin dependence of the physical mechanism that underlies the existing discrepancy. Even the single point at zero degrees would reveal the relative isoscalar to isovector strength of the higher-order mechanism.

ACKNOWLEDGMENTS

C.M.C. and D.J.E. are grateful to the Los Alamos National Laboratory for its kind hospitality during part of the work, while C.M.C. and M.B.J. are similarly grateful to Vanderbilt University. The work of D.J.E. was supported in part by the U.S. Department of Energy under Grant No. DE-FG02-96ER40975. The work of C.M.C. was supported in part by the ROC National Science Council under Grant No. NSC 86-2112-M-129-001.

[1] D. Bugg *et al.*, Phys. Rev. **168**, 1466 (1968); Y. Marlow *et al.*, Phys. Rev. C **25**, 2619 (1982); E. Mardor *et al.*, Phys. Rev. Lett. **65**, 2110 (1990); R. A. Krauss *et al.*, Phys. Rev. C **46**, 655 (1992); R. Sawafta *et al.*, Phys. Lett. B **307**, 293 (1993); R. Weiss *et al.*, Phys. Rev. C **49**, 2569 (1994).

[2] E. Friedman *et al.*, Phys. Rev. C **55**, 1304 (1997).

[3] R. Michael *et al.*, Phys. Lett. B **382**, 29 (1996).

[4] M. J. Páez and R. H. Landau, Phys. Rev. C **24**, 1120 (1981); P. B. Siegel, W. B. Kaufmann, and W. R. Gibbs, *ibid.* **30**, 1256 (1984); C. M. Chen and D. J. Ernst, **45**, 2011 (1992); M. Arima and K. Masutani, **47**, 1325 (1993).

[5] M. F. Jiang, D. J. Ernst, and C. M. Chen, Phys. Rev. C **51**, 857 (1995).

[6] E. Friedman, A. Gal, and J. Mareš, Phys. Lett. B **396**, 21 (1997).

[7] B. C. Clark, S. Hama, G. R. Kälberman, R. L. Mercer, and L. Ray, Phys. Rev. Lett. **55**, 592 (1985).

[8] P. B. Siegel, W. B. Kaufmann, and W. R. Gibbs, Phys. Rev. C **31**, 2184 (1985).

[9] G. E. Brown, C. B. Dover, P. B. Siegel, and W. Weise, Phys. Rev. Lett. **26**, 2723 (1988).

[10] J. C. Caillon and J. Labarosouque, Phys. Lett. B **295**, 21 (1992); **311**, 19 (1993); Nucl. Phys. **A572**, 649 (1994); **A589**, 609 (1995); Phys. Rev. C **53**, 1993 (1995).

[11] C. Garcia-Recio, J. Nieves, and E. Oset, Phys. Rev. C **51**, 237 (1995); U. G. Meissner, E. Oset, and A. Pich, Phys. Lett. B **353**, 161 (1995).

[12] M. F. Jiang and D. S. Koltun, Phys. Rev. C **46**, 2462 (1992).

[13] R. J. Peterson, A. A. Ebrahim, and H. C. Bhang, Nucl. Phys. **A625**, 261 (1997).

[14] D. R. Giebink and D. J. Ernst, Comput. Phys. Commun. **48**, 407 (1988).

[15] D. J. Ernst and G. A. Miller, Phys. Rev. C **21**, 1472 (1980); D. L. Weiss and D. L. Ernst, *ibid.* **26**, 605 (1982); D. R. Giebink, *ibid.* **25**, 2133 (1982).

[16] D. J. Ernst, G. E. Parnell, and C. Assad, Nucl. Phys. **A518**, 658 (1990).

[17] D. J. Ernst and M. B. Johnson, Phys. Rev. C **24**, 2210 (1981).

[18] M. B. Johnson and D. J. Ernst, Phys. Rev. C **27**, 709 (1983); Ann. Phys. (N.Y.) **219**, 266 (1992).

[19] S. J. Greene, C. J. Harvey, P. A. Seidle, R. Gilman, E. R. Siciliano, and M. B. Johnson, Phys. Rev. C **30**, 2003 (1984).

[20] In calculating the total cross section of the deuteron needed to compute *R*, we include the same second order for the deuteron as for the other nuclei. The results are completely independent of this assumption as the deuteron is such a low density that the second order has virtually no effect.

[21] M. F. Jiang and D. J. Ernst, Phys. Rev. C **51**, 1037 (1995).

[22] C. M. Chen, D. J. Ernst, and M. B. Johnson, Phys. Rev. C **48**, 841 (1993).

[23] D. J. Ernst, J. T. Londergan, G. A. Miller, and R. M. Thaler, Phys. Rev. C **16**, 537 (1977).

[24] C. M. Chen, M. B. Johnson, and D. J. Ernst, Phys. Rev. C **58**, 3500 (1998).

[25] M. D. Cooper, M. B. Johnson, and G. B. West, Nucl. Phys. **A292**, 350 (1977).

[26] R. Arndt, computer code SAID, Phys. Rev. D **28**, 97 (1983).

[27] L. Kurth Kerr, B. C. Clark, E. D. Cooper, S. Hama, L. Ray, and G. W. Hoffman (unpublished).

[28] R. J. Peterson (private communication).